J Comp Physiol A
DOI 10.1007/s00359-012-0742-1

ORIGINAL PAPER

Interspecifc variation in eye shape and retinal topography in seven species of galliform bird (Aves: Galliformes: Phasianidae)

Thomas J. Lisney · Andrew N. Iwaniuk · Jeffrey Kolominsky · Mischa V. Bandet · Jeremy R. Corfield · Douglas R. Wylie

Received: 24 April 2012 / Revised: 5 June 2012 / Accepted: 20 June 2012

Abstract Eye morphology and the retinal topography of animals that live in either 'open' (e.g., grassland) or 'enclosed' (e.g., forest) terrestrial habitats show common adaptations to constraints imposed by these different habitat types. Although relationships between habitat and the visual system are well documented in most vertebrates, relatively few studies have examined this relationship in birds. Here, we compare eye shape and retinal topography across seven species from the family Phasianidae (Galliformes) that are diurnally active in either open or enclosed habitats. Species from enclosed habitats have significantly larger corneal diameters, relative to transverse diameters, than species from open habitats, which we predict serves to enhance visual sensitivity. Retinal topography, however, was similar across all seven species and consisted of a centrally positioned *area centralis* and a weak horizontal visual streak, with no discernible fovea. In the Japanese quail (*Coturnix japonica*), there was also a dorso-temporal extension of increased neuron density and, in some specimens, a putative *area dorsalis*. The total number of neurons in the retinal ganglion cell layer was correlated with retinal whole-mount area. Average and peak neuron densities were similar across species, with the exception of the Japanese quail, which had greater average and peak densities. Peak anatomical spatial resolving power was also similar among species, ranging from approximately 10–13 cycles/°. Overall, the pattern of retinal topography we found in phasianids is associated with ground-foraging in birds and presumably facilitates the identification of small food items on the ground as well as other visually guided behaviors, irrespective of habitat type.

Keywords Habitat · Retinal ganglion cell · Spatial resolving power · Terrain theory · Visual ecology

T. J. Lisney (✉) · D. R. Wylie
Department of Psychology, University of Alberta, Edmonton, AB, Canada
e-mail: tomlisney@gmail.com

A. N. Iwaniuk · J. R. Corfield
Department of Neuroscience, Canadian Centre for Behavioural Neuroscience, University of Lethbridge, Lethbridge, AB, Canada

J. Kolominsky · M. V. Bandet · D. R. Wylie
Centre for Neuroscience, University of Alberta, Edmonton, AB, Canada

Introduction

Birds are highly visual animals and most species possess large, well-developed eyes and highly complex retinas (Walls 1942; Meyer 1977; Zeigler and Bischof 1993). Like the eyes of other animals, there is strong evidence that the eyes of birds are adapted to constraints imposed by their ecological niches. For example, many nocturnal birds have the same adaptations for improving visual sensitivity as those found in other animals active in low ambient light levels, such as large eyes, a large corneal diameter relative to total eye size, high rod:cone ratios and high photoreceptor:retinal ganglion cell (RGC) summation ratios (Walls 1942; Oehme 1961; Rojas et al. 2004; Warrant 2004; Corfield et al. 2011). In contrast, the eyes of diurnal raptors, such as eagles and kestrels, have adaptations that improve visual resolution including well-developed central and temporally positioned foveae containing very large numbers of cones and low photoreceptor:RGC summation ratios in the perifoveal regions (Fite and Rosenfield-Wessels 1975; Reymond 1985, 1987; Inzunza et al. 1991). There is also some evidence that birds conform to Hughes' (1977)

Published online: 18 July 2012

'terrain' theory, which posits that there is a close relationship between the topographic distribution of RGCs across the retina and the symmetry or 'openness' of a species' habitat (Hughes 1975, 1977; Collin 1999, 2008). The retinas of birds that live in 'open' habitats dominated by an unobstructed horizon, such as grasslands, tundra, deserts and the open ocean, are characterized by a well-defined visual streak, which is an elongated area of increased RGC density stretching across the horizontal retinal meridian (Hayes and Brooke 1990; Boire et al. 2001; Fernández-Juricic et al. 2011a; Lisney et al. 2012). This retinal specialization is thought to allow an animal a panoramic view of its visual field, without the need for extensive eye or head movements (Hughes 1977; Collin 1999, 2008). In contrast, in 'enclosed' habitats, such as forests and woodland, as well as at night, the visual horizon is obscured by vegetation and/or darkness. Birds that predominantly live in enclosed habitats and/or exhibit nocturnal activity patterns lack a distinct visual streak and instead possess a more radially symmetrical retinal topography (that is sometimes referred to as a 'weak' visual streak) containing one or more high density areas for acute vision (termed *areae*), which may or may not be foveated (Hayes and Brooke 1990; Collin 1999, 2008; Rahman et al. 2007; Dolan and Fernández-Juricic 2010; Fernández-Juricic et al. 2011b; Lisney et al. 2012). Without the advantage of perceiving a panoramic visual field with high acuity offered by a well-defined visual streak, species that live in enclosed habitats must rely on increased eye and/or head movements in order to accurately align their *areae* upon objects of interest (Collin 1999, 2008).

These generalizations are, however, based on the study of a relatively small number of avian species. Little is known about the anatomical organization of the eye and retina in most birds, and so the extent to which the visual systems of birds from the same order or family vary according to habitat is not well understood. In this study, we focus on eye shape and RGC topography in several species from the family Phasianidae (Order Galliformes). This family includes the domestic chicken (*Gallus gallus*), pheasants, partridges, grouse and Old World quails. All of the species within this family are ground dwellers, poor fliers and feed on similar food items (such as seeds, grains, shoots and insects), regardless of habitat (del Hoyo et al. 1994). Although the visual systems of the chicken and Japanese quail (*Coturnix japonica*) have been studied in detail (e.g., Meyer and May 1973; Ehrlich 1981; Morris 1982; Budnik et al. 1984; Ikushima et al. 1986; Foster et al. 1987; Straznicky and Chehade 1987; Schaeffel and Howland 1989; Chen and Naito 1999), relatively little is known about the visual system of other phasianids (but see Hart 2002). All phasianids are diurnally active, but live in a variety of open (e.g., prairie grassland, cultivated fields, rocky mountainsides) and enclosed (woodland and forest) habitats (Johnsgard 1973; del Hoyo et al. 1994). Given that eye morphology and retinal topography in vertebrates often vary with ambient light levels and habitat, we expected that eye shape and retinal topography would differ between phasianids from open and enclosed habitats. More specifically, because light intensity levels at the forest floor can be over 100–200 times lower than at ground level in open habitats at the same time of day (Ovington and Madgwick 1955; Martin 1982; Endler 1993), we predicted that species in enclosed habitats would have relatively large corneal diameters, which would improve visual sensitivity (Walls 1942; Kirk 2004, 2006). We also predicted that phasianids would conform to the terrain theory (Hughes 1977), such that species living in open habitats will have a well-defined, elongated visual streak, and species that live in enclosed habitats will have a less well-defined, weak visual streak. Our results suggest that while eye shape does differ among phasianids in relation to habitat type, retinal topography is highly conserved and shows little interspecific variation.

Materials and methods

Study species

We examined eyes from seven phasianid species (Crowe et al. 2006; Kolm et al. 2006): the chukar partridge (*Alectoris chukar*), the ruffed grouse (*Bonasa umbellus*), the Japanese quail (*C. japonica*), the spruce grouse (*Falcipennis canadensis*), the gray partridge (*Perdix perdix*), the ring-necked pheasant (*Phasianus colchicus*) and the sharp-tailed grouse (*Tympanuchus phasianellus*). In order to compare among species, we divided phasianid habitats into two broad categories, 'enclosed' and 'open' (Collin and Pettigrew 1988a, b, 1989; Collin 1999; Ahnelt et al. 2006). The ruffed and spruce grouse live in enclosed deciduous and coniferous forest habitats, respectively, while the other five species prefer more open habitats, such as prairie grassland, bare rocky slopes and agricultural land (Johnsgard 1973; del Hoyo et al. 1994). Compared to the forest habitats of the ruffed and spruce grouse, these open habitats contain a distinct horizon and experience relatively higher ambient light levels due to the lack of a canopy. This applies even if seasonal variations (such as changes in leaf cover, hours of daylight and the position of the sun in the sky) are taken into account (Ovington and Madgwick 1955). Ruffed grouse were caught in mirror traps (Gullion 1965) during the breeding season in central Alberta, Canada, killed with an intraperitoneal injection of sodium pentobarbital (100 mg kg^{-1}) and the eyes and heads were immersion fixed in 4 % buffered (pH 7.4) paraformaldehyde.

The Japanese quail were purchased from a commercial supplier and subjected to the same protocols as the ruffed grouse. For all of the remaining species, we obtained eyes from hunters and falconers, which were immersion fixed using the same fixative within 30 min of death. The gray partridge and ring-necked pheasant are not native species in Alberta and are the progeny of animals introduced from Eurasia in the nineteenth and twentieth centuries (Johnsgard 1973; del Hoyo et al. 1994). Both species, however, inhabit similar habitats in North America to those in their native locations (Christensen 1970; Johnsgard 1973; del Hoyo et al. 1994). Chukar partridge are also endemic to Eurasia and are not currently found in Alberta, but are frequently released as game birds on private properties. Our specimens were obtained from hunters on these properties.

Eye morphology

From 26 individual birds, 42 eyes were used. Each eye was cleaned of all fascia and extraocular musculature. Transverse diameters of the eye and the cornea were then measured to the nearest 0.01 mm using digital calipers along two perpendicular planes (Fig. 1a). This yielded a maximum and a minimum for both transverse eye diameter and corneal diameter. Eye shape was then quantified by calculating the ratio of mean corneal diameter to mean transverse eye diameter (*C*:*T* ratio; Kirk 2004, 2006). The *C*:*T* ratio is a measure of the size of the cornea relative to the theoretical maximal corneal diameter that could be obtained in an eye of a fixed size (i.e., a corneal diameter equal to transverse eye diameter) (Kirk 2004, 2006). The size of the cornea places an upper limit on the maximum size of the pupillary aperture and thus the amount of light that can enter the eye and, as mentioned previously, animals active in low ambient light levels have been consistently shown to have large corneas relative to total eye size (Walls 1942; Hughes 1977; Pettigrew et al. 1988; Kirk 2004, 2006; Hall and Ross 2007; Schmitz and Wainwright 2011; Veilleux and Lewis 2011; Lisney et al. 2012).

In previous studies where eye shape has been determined in a similar fashion, the eye and corneal diameter measurements have been made from eyes that were 'reinflated' with fixative using a syringe and a small-gauge needle (e.g., Kirk 2004, 2006; Hall and Ross 2007; Lisney et al. 2012). Eyes are reinflated until they return to a globose shape and resist further attempts at inflation, thus reflecting the shape of the living eye. In this study, the majority of the eyes (71 %) could not be reinflated because of small cuts in the sclera that occurred during the dissection process, or because small cuts were purposely made in the sclera to facilitate the infusion of fixative into the vitreous chamber. These eyes had collapsed to varying extents in the axial plane (due to loss of internal fluids postmortem; Kirk 2004), but in the transverse plane the eyes still closely resembled the shape of eyes that could be reinflated. Therefore, we predicted that our measurements of corneal and eye transverse diameter should be the same, irrespective of whether an eye could be reinflated or not. This was confirmed by comparing *C*:*T* ratios calculated from corneal and eye diameter measurements made before and after reinflation from the 12 eyes that could be reinflated. A Wilcoxon test for matched pairs revealed no significant difference in the *C*:*T* ratios calculated using before and after reinflation measurements ($W = -14$, $P = 0.577$). Furthermore, using the approach described in Lessells and Boag (1987), we calculated a high level of repeatability (r) for the before and after reinflation measures of *C*:*T* ratio ($r = 0.831$).

The axial length (A) of the eye was also measured for the eyes that could be reinflated (Fig. 1b). These values were used in the calculation of peak anatomical spatial resolving power (see below) and also to calculate a second eye morphology ratio, the *C*:*A* ratio (Kirk 2006; Veilleux and Lewis 2011). The *C*:*A* ratio reflects the size of the cornea relative to axial length. Axial length is a proxy of focal length, which in turn is directly proportional to retinal image size and inversely proportional to retinal image brightness (Kirk 2006). Both *C*:*T* and *C*:*A* ratios are measures of cornea size relative to total eye size (Kirk 2006) and animals that live in dim light exhibit consistently higher values for both ratios compared to animals that live in higher light levels (Pettigrew et al. 1988; Kirk 2004, 2006; Hall and Ross 2007; Schmitz and Wainwright 2011; Veilleux and Lewis 2011; Lisney et al. 2012).

Retinal whole mounts

Each eyeball was hemisected and the retina was dissected out of the scleral eyecup. During this process, the condition of each retina was assessed. Some of the retinas were significantly torn or folded, or were so fragile that they fell apart as soon as they were touched with a paint brush or a pair of fine forceps. These retinas were not in acceptable condition for whole mounting and so were not processed further. Of the 42 eyes, 23 of the retinas were of an acceptable condition for whole mounting, meaning they were dissected intact. The retinal pigment epithelial layer was bleached for 24 h at room temperature using a solution of 20 % hydrogen peroxide in phosphate-buffered saline (Lisney et al. 2012). Each retina was cleared of vitreous, had the pecten cut off at the base or removed entirely, and was whole mounted, with the RGC layer uppermost, onto a gelatinized slide coated with Fol's mounting medium before being defatted in Citrisolv (Fisher Scientific), rehydrated through a descending alcohol series followed by distilled water and stained for Nissl substance in an

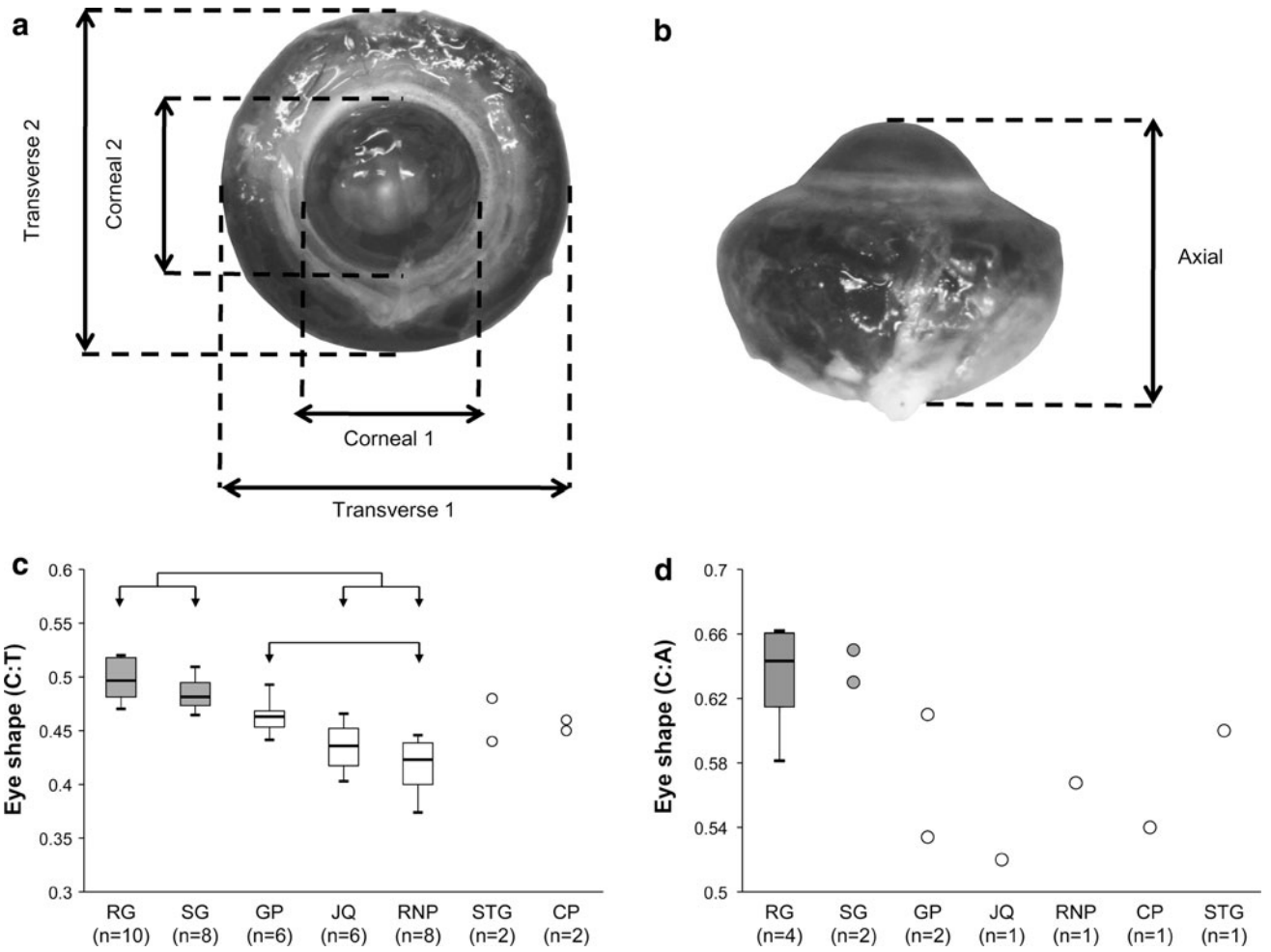

Fig. 1 Eye morphology in phasianid birds. **a** Dorsal and **b** lateral views of an eye from a spruce grouse (*Falcipennis canadensis*), illustrating the measurements of **a** corneal and eye transverse diameter, and **b** eye axial length. Eye axial length was only measured in eyes that could be reinflated. **c**, **d** *Box* and *whisker plots* showing interspecific variation in eye shape using the ratio of mean corneal diameter to mean transverse eye diameter (*C*:*T*) (**c**) and the ratio of mean corneal diameter to axial eye diameter (*C*:*A*) (**d**). *CP* chukar partridge (*Alectoris chukar*), *GP* gray partridge (*Perdix perdix*), *JQ* Japanese quail (*Coturnix japonica*), *RNP* ring-necked pheasant (*Phasianus colchicus*), *RG* ruffed grouse (*Bonasa umbellus*), *SG* spruce grouse (*Falcipennis canadensis*), *STG* sharp-tailed grouse (*Tympanuchus phasianellus*). The two species from enclosed habitats (the ruffed and spruce grouse) are shown in *gray*. The other five species that live in open habitats are shown in *white*. *Arrow bars* represent significant ($P \leq 0.05$) differences from pair-wise multiple comparisons tests

aqueous solution of 0.1 % Cresyl Violet (pH 4.3). After staining, each retina was rinsed in distilled water and dehydrated through an ascending alcohol series, cleared in Citrisolv and coverslipped with Permount (Stone 1981; Ullmann et al. 2012; Lisney et al. 2012).

Shrinkage of the retinal whole mounts was assessed as in Lisney et al. (2012). Briefly, scaled digital photographs of each whole mount were taken before and after staining and the outline of each whole mount was traced using the public domain NIH image program ImageJ (Rasband 1997–2011). Whole mount shrinkage was, on average, 8.6 ± 4.6 % and was confined to the margins of the whole mount and along the edges of the radial relieving cuts or tears (Stone 1981).

Neuron counts

The neurons in the RGC layer of each whole mount were counted using systematic random sampling using fractionator principle (Gundersen 1977). Digital photo-micrographs of the RGC layer were taken at regular intervals as defined by a sampling grid measuring 0.75 × 0.75 or 1 × 1 mm (depending on whole mount area) using a × 100 oil immersion objective (NA = 1.3) on a Leica DMRE compound microscope with a Retiga EXi *FAST* Cooled mono 12-bit camera (Qimaging, Burnaby, B.C., Canada) and OPENLAB Imaging system (Improvision, Lexington, MA, USA). The *X*–*Y* coordinates of each point on the sampling grid were determined using the *X*–*Y*

Vernier scales on the microscope's stage. Nissl-stained neurons were counted using an unbiased counting frame (35 × 35 μm) (Gundersen 1977) that was imposed upon each digital photo-micrograph using ImageJ. Only glial cells, which were distinguished on the basis of their small size, elongate 'spindle'- or 'cigar'-like shape and dark staining (Fig. 2) (Hughes 1985; Wathey and Pettigrew 1989; Coimbra et al. 2009) were omitted from the counts. This means that the population of 'displaced' amacrine cells that is found in the RGC layer was included in the counts, and thus our counts likely represent an overestimation of the true RGC densities. Although some authors have used cytological criteria to distinguish between RGCs and amacrine cells in avian retinas (e.g., Ehrlich 1981; Hayes and Brooke 1990; Inzunza et al. 1991; Hart 2002; Dolan and Fernández-Juricic 2010), we were unable to unequivocally discern RGCs from amacrine cells using these criteria in areas of high neuron density in our specimens. Therefore, in order avoid any issues associated with differentiating amacrine cells from RGCs, such as the misidentification of small RGCs, our retinal topography maps and data are based on counts of all Nissl-stained neurons in the RGC layer, as described above (Hughes 1977; Stone 1981; Collin and Pettigrew 1988a, b; Wathey and Pettigrew 1989; Lisney and Collin 2008; Coimbra et al. 2009; Lisney et al. 2012).

The neuron counts for each counting frame were converted to density counts in cells mm^{-2}. For each retina, the total number of neurons in the RGC layer was determined by multiplying the total number of sampled cells by the inverse of the area-sampling fraction (asf), which is equal to the area of the counting frame divided by the area of the sampling grid (Howard and Reed 2005). Coefficients of error (CE) were calculated using Scheaffer's estimator for a one-stage systematic sample (Schaeffer et al. 1996) for non-homogeneous distributions (Schmitz and Hof 2000). Our CEs were all ≤ 0.029, thereby indicating that our estimates of the total number of neurons in the RGC layer are robust (Boire et al. 2001; Coimbra et al. 2009; Ullmann et al. 2012).

To construct retinal topography maps, the density counts for each sample point were entered into DeltaGraph 6 (Red Rock Software, Salt Lake City, UT, USA) and an interpolated isodensity contour plot was created, following Ahnelt et al. (2006) and Schiviz et al. (2008). The scaled, correctly oriented outline of each whole mount, traced from a digital photograph (see above), was then superimposed on top of the contour plot to complete the topography map.

Spatial resolving power

The theoretical peak anatomical spatial resolving power (SRP) of each species was calculated using peak RGC layer neuron density values in combination with a measure of the focal length of the eye, the posterior nodal distance (PND; the distance from the lens center to the choroid–retina border) (Ullmann et al. 2012). PND was estimated from eye axial length, which was measured using eyes that were reinflated (see above). At least one eye was successfully reinflated for each species. The PND was then taken to be × 0.6 of the eye axial length (Hughes 1977; Martin 1994; Ullmann et al. 2012). Assuming a hexagonal retinal mosaic (Hart 2002), the distance (d) subtended by 1 ° on the retina was calculated:

$$d = \frac{2\pi f}{360} \quad (1)$$

The cell-to-cell spacing (S) of neurons in the RGC layer was determined using the formula:

$$S^2 = \frac{2}{(D\sqrt{3})} \quad (2)$$

where D is the peak neuron density in mm^{-2}. The maximum spatial (Nyquist) frequency (v) of a grating resolvable by this arrangement (Synder and Miller 1977) was calculated as:

$$v = \frac{1}{(S\sqrt{3})} \quad (3)$$

To express SRP in cycles/°, the value of v was multiplied by d.

Statistical analysis

Statistical analyses were performed using Prism 4 (GraphPad Software, San Diego, CA, USA). After confirming the data were normally distributed and exhibited homogeneity of variance, one-way ANOVA was used to test for significant differences in eye shape (C:T ratio) among the species. Bonferroni multiple comparison tests were also used to evaluate pair-wise differences in eye shape between species. Non-parametric statistical tests (Kruskal–Wallis tests adjusted for tied ranks and Dunn's multiple comparisons tests) were used to test for significant differences in total, peak and average neuron density, as well as SRP, among species. Only species for which four retinas were analyzed were included in the multiple comparisons tests. Although non-parametric tests are generally less powerful than corresponding parametric tests, they do not assume that the data are normally distributed (Fowler and Cohen 1990; Quinn and Keough 2002). Because our retinal topography data consisted of small sample sizes ($n \leq 4$ for all species), we erred on the side of caution and opted to use non-parametric tests as it was not possible to determine whether our data were normally distributed. Spearman rank correlation coefficients were used to test

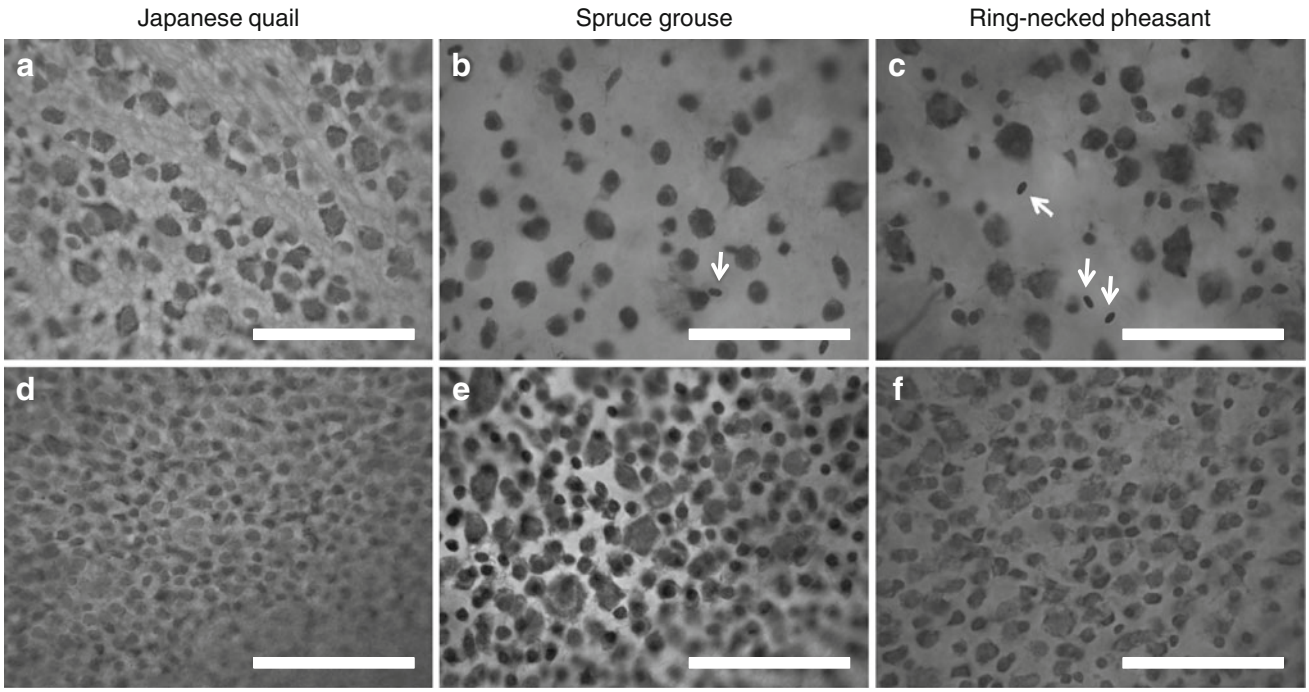

Fig. 2 High power digital photo-micrographs showing Nissl-stained cells in the retinal ganglion cell layer in three species, the Japanese quail (*Coturnix japonica*) (**a**, **d**), ruffed grouse (*Bonasa umbellus*) (**b**, **e**) and ring-necked pheasant (*Phasianus colchicus*) (**c**, **f**). **a–f** Relatively lower (4,080–8,160 cells mm^{-2}) and higher (17,100–27,800 cells mm^{-2}) cell densities, respectively. Examples of glial cells, which were distinguished on the basis of their small size, elongate 'spindle'- or 'cigar'-like shape and dark staining, are *arrowed*. *Scale bars* represent 50 μm

correlations between *C*:*A* and *C*:*T* ratios, and whole mount area and total neuron number.

Results

Eye shape

The two species from enclosed habitats, the ruffed and spruce grouse, had the largest average *C*:*T* ratios (0.5 and 0.49, respectively), while the other five open habitat species had average *C*:*T* ratios ranging from 0.42 to 0.46 (Table 1; Fig. 1c). A one-way ANOVA yielded a significant difference in mean *C*:*T* ratio among species ($F_{4,33} = 19.47$, $P < 0.0001$). Bonferroni multiple comparison tests showed that both the ruffed and spruce grouse had a significantly different eye shape than the Japanese quail and the ring-necked pheasant ($P \leq 0.01$), while the gray partridge also had a significantly different eye shape to the ring-necked pheasant ($P < 0.01$).

A similar trend was seen in the *C*:*A* ratios. The *C*:*A* ratios were, on average, higher for both of the species from enclosed habitats (0.63), compared to the five species from open habitats (0.52–0.6) (Table 1; Fig. 1d). Because of the small sample sizes ($n = 1$–2 for most species), these differences were not tested statistically, but average *C*:*A* ratios were significantly correlated with average *C*:*T* ratios (Spearman $r = 0.817$, $P = 0.034$).

Retinal topography maps

The density of neurons in the RGC layer varied across the retina in all seven species (Table 1; Figs. 2, 3, 4). The neuron densities ranged from approximately 2,000–3,000 cells mm^{-2} in the lowest density areas in most species (ca. 7,000 cells mm^{-2} in the Japanese quail) to around 22,000–29,000 cells mm^{-2} in the highest density areas, again with the exception of the Japanese quail (ca. 35,000 cells mm^{-2}). We have tentatively termed the highest density area in all species an *area centralis*, because we could not confirm the presence of a foveal pit in any of our whole mounts. Representative isodensity contour retinal topography maps for each species are shown in Fig. 3. These maps show that the retinal topography pattern was similar among all seven species, and thus there were no differences in retinal topography between species from enclosed and open habitats. In all the species, the *area centralis* was located in the central retina, just dorsal to the superior pole of the pecten. Also, the isodensity contours were relatively loosely packed and

Table 1 Summary of eye morphology and retinal topography for seven species of phasianid bird that live in either enclosed or open habitats

Species	*Bonasa umbellus*	*Falcipennis canadensis*	*Perdix perdix*	*Coturnix japonica*	*Phasianus colchicus*	*Alectoris chukar*	*Tympanuchus phasianellus*
Common name	Ruffed grouse	Spruce grouse	Gray partridge	Japanese quail	Ring-necked pheasant	Chukar partridge	Sharp-tailed grouse
Habitat type	Enclosed	Enclosed	Open	Open	Open	Open	Open
Eye morphology							
Average eye transverse diameter (*T*) (mm, ± SD)	17.57 ± 0.31 ($n = 10$)	17.14 ± 0.80 ($n = 8$)	14.50 ± 0.22 ($n = 6$)	10.98 ± 4.84 ($n = 6$)	19.44 ± 0.69 ($n = 8$)	15.60 ($n = 2$)	17.72 ($n = 2$)
Average corneal diameter (*C*) (mm, ± SD)	8.77 ± 0.26 (n = 10)	8.33 ± 0.51 ($n = 8$)	6.70 ± 0.30 ($n = 6$)	4.84 ± 0.31 ($n = 6$)	8.24 ± 0.57 ($n = 8$)	7.11 ($n = 2$)	7.86 ($n = 2$)
Eye shape (*C*:*T*) (± SD)	0.50 ± 0.02 ($n = 10$)	0.49 ± 0.02 ($n = 8$)	0.46 ± 0.02 ($n = 6$)	0.44 ± 0.02 ($n = 6$)	0.42 ± 0.02 ($n = 8$)	0.46 ($n = 2$)	0.44 ($n = 2$)
Eye axial diameter (*A*) (mm)	13.73 ± 0.98 ($n = 4$)	13.25 ($n = 2$)	12.1 ($n = 2$)	9.33 ($n = 1$)	13.98 ($n = 1$)	13.3 ($n = 1$)	13.65 ($n = 1$)
Eye shape (*C*:*A*) (± SD)	0.63 ± 0.04 ($n = 4$)	0.63 ($n = 2$)	0.57 ($n = 2$)	0.52 ($n = 1$)	0.57 ($n = 1$)	0.53 ($n = 1$)	0.60 ($n = 1$)
Retinal topography							
Peak neuron density (cells mm^{-2}, ± SD)	24,725 ± 3,428 ($n = 4$)	22,050 ± 3,269 ($n = 4$)	22,450 ± 3,371 ($n = 4$)	35,115 ± 5,218 ($n = 4$)	26,964 ± 1,061 ($n = 4$)	24,450 ($n = 2$)	28,800 ($n = 1$)
Total number of neurons (± SD)	2,659,592 ± 266,333 ($n = 4$)	2,816,122 ± 319,730 ($n = 4$)	1,634,490 ± 141, 402 ($n = 4$)	1,508,648 ± 74, 888 ($n = 4$)	3,311,225 ± 161, 300 ($n = 4$)	2,292,653 ($n = 2$)	2,999,184 ($n = 1$)
CE (± SD)	0.027 ± 0.004 ($n = 4$)	0.022 ± 0.002 ($n = 4$)	0.029 ± 0.003 ($n = 4$)	0.027 ± 0.004 ($n = 4$)	0.026 ± 0.002 ($n = 4$)	0.028 ($n = 2$)	0.023 ($n = 1$)
Whole mount area (mm^2)	262.2 ± 6.1 ($n = 4$)	302.1 ± 14.9 ($n = 4$)	178.2 ± 22.6 ($n = 4$)	98.4 ± 11.8 ($n = 4$)	373.6 ± 37.5 ($n = 4$)	251.9 ($n = 2$)	262.3 ($n = 1$)
Average neuron density (cells mm^{-2}, ± SD)	10,000 ± 877 ($n = 4$)	9,345 ± 1,229 ($n = 4$)	9,221 ± 638 ($n = 4$)	15,443 ± 1,886 ($n = 4$)	9,000 ± 1,300 ($n = 4$)	8,703 ($n = 2$)	11,434 ($n = 1$)
Spatial resolving power							
Eye axial diameter (mm)	13.73 ± 0.98 ($n = 4$)	13.25 ($n = 2$)	12.10 ($n = 2$)	9.33 ($n = 1$)	13.98 ($n = 1$)	13.30 ($n = 1$)	13.65 ($n = 1$)
PND (mm)	8.24 ± 0.59 ($n = 4$)	7.95 ($n = 2$)	7.26 ($n = 2$)	5.60 ($n = 1$)	8.39 ($n = 1$)	7.98 ($n = 1$)	8.19 ($n = 1$)
SRP (cycles/°)	12.1 ± 0.9 ($n = 4$)	11.0 ± 0.8 ($n = 4$)	10.2 ± 0.8 ($n = 4$)	9.7 ± 0.7 ($n = 4$)	12.9 ± 0.3 ($n = 4$)	11.7 ($n = 2$)	13.0 ($n = 1$)

Values for individual eyes and average values are presented, along with ± 1 SD for the species for which data for three or more eyes were available. The number of eyes/retinas assessed for each species (n) is given in parentheses

CE coefficients of error for the estimates of the total numbers of neurons in the retinal ganglion cell layer, *PND* posterior nodal distance, *SRP* spatial resolving power

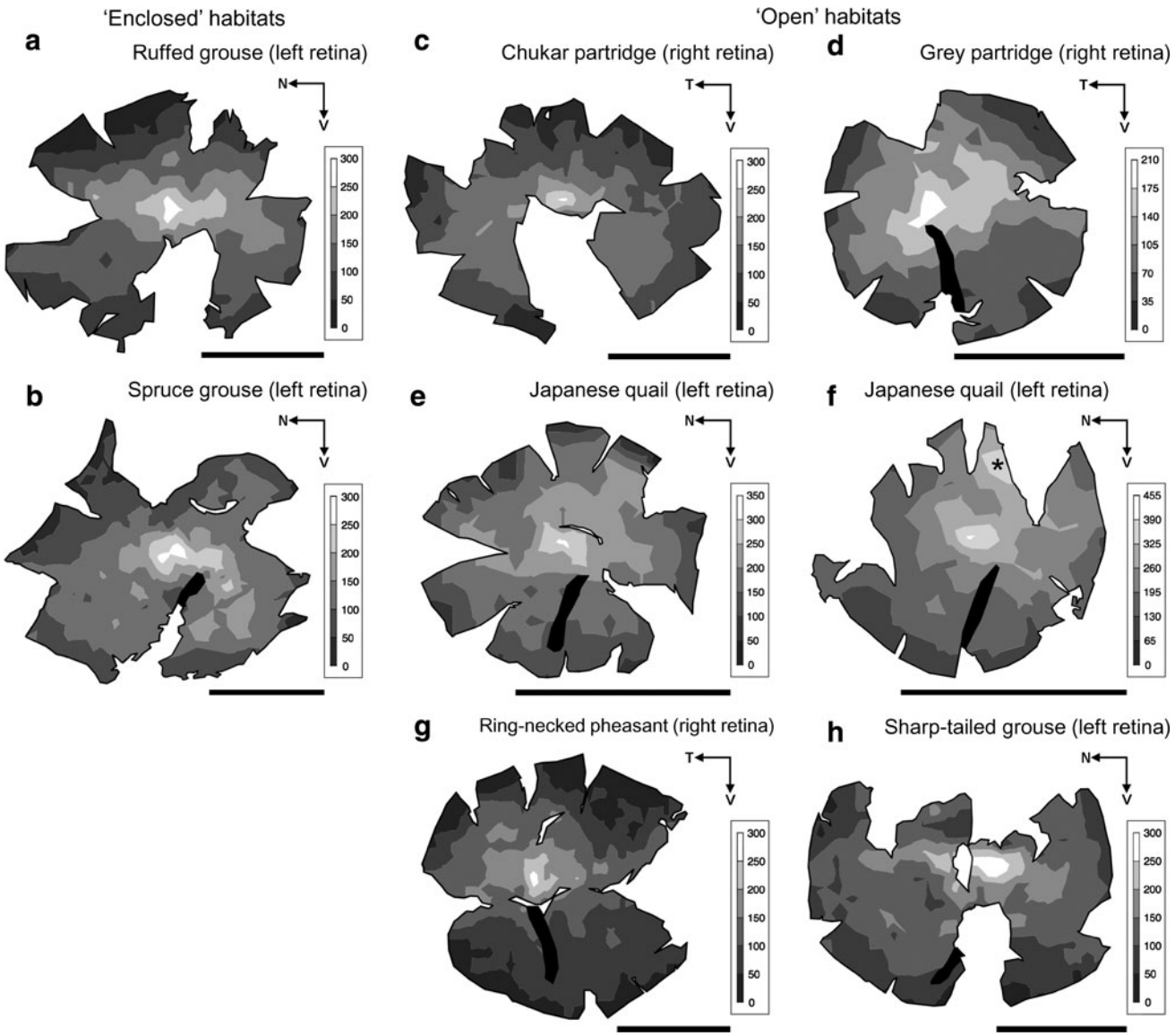

Fig. 3 Representative isodensity contour retinal topography maps illustrating the distribution of neurons in the retinal ganglion cell layer for seven species of galliform bird from 'enclosed' (**a**, **b**) and 'open' habitats (**c–h**). **a** Left retina from a ruffed grouse (*Bonasa umbellus*). **b** Left retina from a spruce grouse (*Falcipennis canadensis*). **c** Right retina from a chukar partridge (*Alectoris chukar*). **d** Right retina from a gray partridge (*Perdix perdix*). **e**, **f** Two left retinas from Japanese quail (*Coturnix japonica*). **g** Right retina from a ring-necked pheasant (*Phasianus colchicus*). **h** Left retina from a sharp-tailed grouse (*Tympanuchus phasianellus*). In all species, an *area centralis* was located in the central retina, just dorsal to the superior pole of the pecten and the isodensity contours formed a weak horizontal visual streak. In the Japanese quail, there was a dorso-temporal extension of increased neuron density (**e**, **f**), and in some Japanese quail whole mounts, a second, putative high density area was identified in the dorso-temporal retina (*asterisk*), which may be an *area dorsalis* (**f**). The *shaded* density scales, which are different among species, represent × 10 E03 cells mm^{-2}. The *irregular black* shapes in **b** and **d–g** represent the position of the pecten. *Scale bars* represent 10 mm. *N* nasal, *T* temporal, *V* ventral

generally horizontally aligned in all the whole mounts, forming a weak horizontal visual streak. In the Japanese quail, there was also a dorso-temporal extension of increased neuron density (Fig. 3e, f), and in two of the four Japanese quail whole mounts, a second, putative high density area was identified in the dorso-temporal retina, which may be an *area dorsalis* (Fig. 3f).

Neuron number and SRP

As mentioned above, the peak neuron densities were similar for all species except for the Japanese quail (Fig. 4a). A Kruskal–Wallis test yielded a significant difference among species ($\chi^2 = 12.42$, $P = 0.0145$), while Dunn's multiple comparisons tests revealed a significant difference

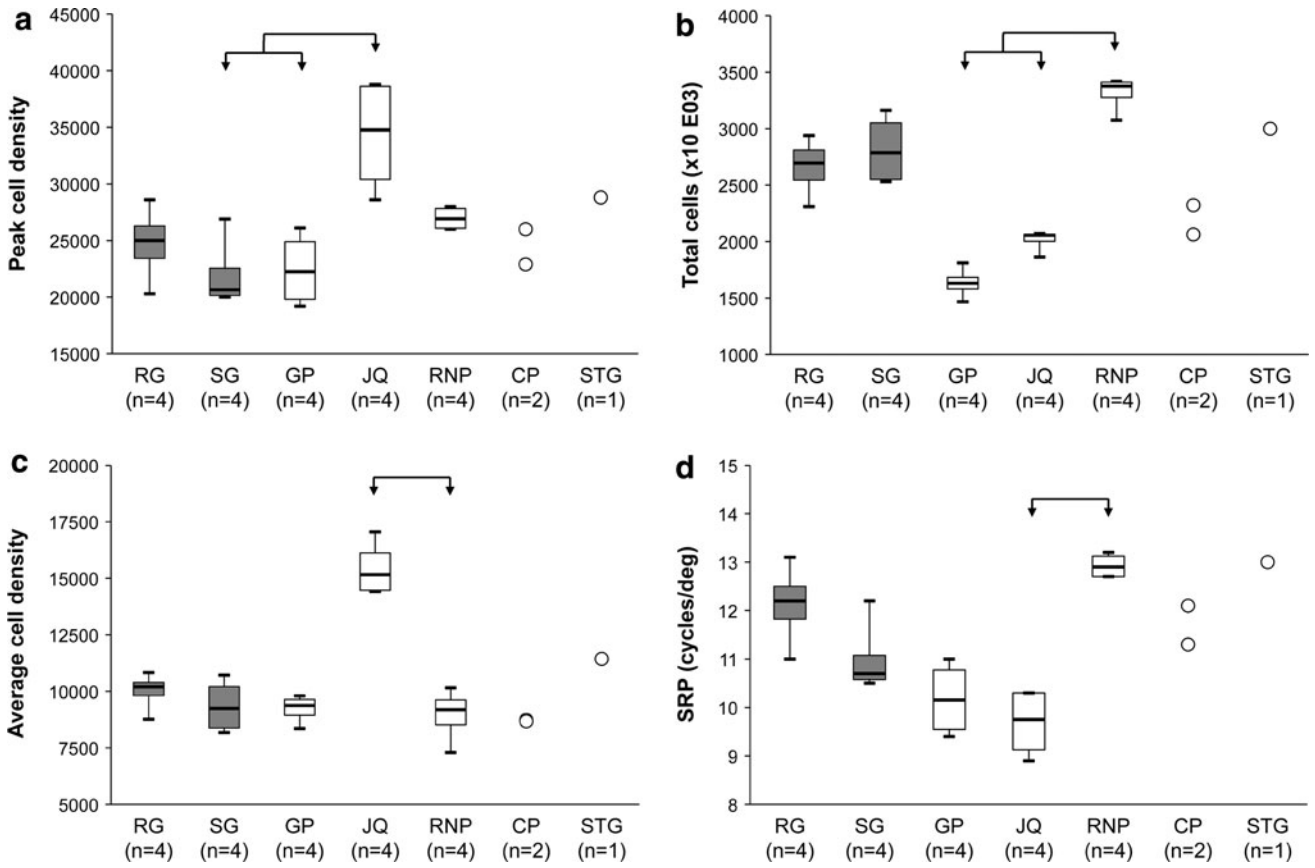

Fig. 4 *Box* and *whisker plots* showing interspecific variation in the peak (**a**) and average (**c**) densities and total numbers (**b**) of neurons in the retinal ganglion cell layer and peak anatomical spatial resolving power (SRP) (**d**) in seven species of phasianid bird. Species abbreviations and shading are the same as in Fig. 1. The two species from enclosed habitats (the ruffed and spruce grouse) are shown in *gray*. The other five species that live in open habitats are shown in *white*. *Arrow bars* represent significant ($P \leq 0.05$) differences from pair-wise multiple comparisons tests

in peak neuron density between the Japanese quail and spruce grouse ($P < 0.05$) and the gray partridge ($P < 0.05$).

The total numbers of neurons in the RGC layer ranged from 1,508,648 in the Japanese quail to 3,311,225 in the ring-necked pheasant (Table 1; Fig. 4b). There was a significant difference among species (Kruskal–Wallis $\chi^2 = 16.57$, $P = 0.0023$), while Dunn's multiple comparisons tests revealed significant differences between the ring-necked pheasant and both the gray partridge ($P < 0.05$) and the Japanese quail ($P < 0.01$). The total number of neurons in the RGC layer was significantly correlated with whole mount area (Spearman $r = 0.911$, $P < 0.0001$).

The average neuron densities were similar in most species, ranging from ca. 8,700 to 10,000 cells mm^{-2} (Table 1; Fig. 4c), with the exception of the Japanese quail, which had approximately $\times$ 1.5 the neuronal density of the other species. There was a significant difference among species (Kruskal–Wallis $\chi^2 = 11.10$, $P = 0.0255$) and Dunn's multiple comparisons tests showed a significant difference in average neuron density between the ring-necked pheasant and the Japanese quail ($P < 0.05$).

Theoretical peak anatomical SRP ranged from an average of 9.7 cycles/° in the Japanese quail to 13.0 cycles/° in the sharp-tailed grouse (Table 1; Fig. 4d). A significant difference in SRP among species was detected (Kruskal–Wallis $\chi^2 = 15.26$, $P = 0.0042$), while Dunn's multiple comparisons tests showed a significant difference in SRP between the ring-necked pheasant and the Japanese quail ($P < 0.01$).

We found no evidence of differences in peak and average neuron density, total neuron number or peak SRP between species from enclosed and open habitats.

Discussion

Overall, our results indicate that phasianids living in enclosed habitats have relatively larger corneal diameters than those living in open habitats, but there are no habitat

related differences in retinal topography, number or density of neurons in the RGC layer or in spatial resolving power. Thus, phasianids are similar to other vertebrates in terms of the association between eye shape and habitat (Schmitz and Wainwright 2011; Veilleux and Lewis 2011), but do not appear to adhere to the terrain theory (Hughes 1977). As well as having the centrally positioned *area centralis* and a weak visual streak common to all of the phasianids investigated, the Japanese quail also has a dorso-temporal extension of increased neuron density and, in some specimens, a putative *area dorsalis*.

Eye shape

Vertebrate eye shape is closely related to the ambient light levels under which different species are active; species active in dim light have larger corneal diameters relative to eye axial length than diurnal species, and crepuscular/cathemeral species have an intermediate eye shape (Walls 1942; Hughes 1977; Pettigrew et al. 1988; Kirk 2004; Hall and Ross 2007; Schmitz and Wainwright 2011; Veilleux and Lewis 2011; Lisney et al. 2012). The size of the cornea places an upper limit on the maximum size of the pupillary aperture and thus the amount of light that can enter the eye. Thus a large corneal area, in combination with large radius of curvature for both the cornea and the lens, serves to improve visual sensitivity by enabling animals that live in dim light to maximize the brightness of the image on their retinas (Walls 1942; Kirk 2004, 2006). As well as the major differences ($\times$ 1 million or greater; Martin 1982) in ambient light levels that occur between day and night, ambient light levels can also vary to a lesser extent (ca. $\times$ 100–200) between open grassland and enclosed forest habitats at the same time of day, as a result of the shading effect of the canopy (Ovington and Madgwick 1955; Martin 1982; Endler 1993). As mentioned previously, this distinction applies even if seasonal variation is taken into account (Ovington and Madgwick 1955). Whether this difference in ambient light levels between open and enclosed habitats is large enough to influence eye shape in vertebrates is not well studied, but recent work on mammals has shown that species that live in enclosed habitats and experience lower light levels have relatively enlarged corneal diameters compared to species from open habitats (Veilleux and Lewis 2011).

Here, we have found a similar relationship between habitat and eye shape in phasianid birds. Although all of the species we investigated are diurnally active, the ruffed and spruce grouse, which both live in enclosed (and therefore relatively dimmer) habitats, have larger *C*:*T* and *C*:*A* ratios compared to species that live in open habitats. As in mammals (Veilleux and Lewis 2011), this likely confers enhanced visual sensitivity in both species. This could be of particular benefit to ruffed grouse, which although diurnally active, often engage in their courtship displays at night and several hours before sunrise (Archibald 1976; Iwaniuk, unpublished data). While other phasianid species also partake in courtship activity before sunrise (Bergerud and Gratson 1988), compared to ruffed grouse their lek sites are in more open habitats. In contrast, ruffed grouse courtship display is dependent on locating a specific log on the forest floor under the cover of darkness (Gullion 1984). Therefore, enhanced visual sensitivity would likely enable them to navigate more effectively under scotopic conditions and potentially avoid nocturnally active predators, such as foxes (*Vulpes vulpes*), coyotes (*Canis latrans*) and owls.

Retinal topography

The RGCs represent the primary output of the eye because their axons project directly to the brain. The displaced amacrine cells that are also found in the RGC layer do not, however, contribute an axon to the brain optic nerve and are not part of the RGC sampling array. Because we did not differentiate between RGCs and amacrine cells in this study, we have likely overestimated RGC densities in phasianid birds. Nevertheless, it is unlikely that the inclusion of amacrine cells in our study significantly affected our findings (Pettigrew et al. 1988, 2010; Pettigrew and Manger 2008). It is common practice to assess retinal topography using counts of all the Nissl-stained neurons in the RGC layer, as we have done (e.g., Hughes 1977; Stone 1981; Collin and Pettigrew 1988a, b; Wathey and Pettigrew 1989; Coimbra et al. 2009; Lisney et al. 2012), especially given the difficulties associated with differentiating between RGCs and amacrine cells in Nissl-stained material, or using retrograde-labeling techniques to specifically label the RGCs (Collin and Pettigrew 1988c; Collin et al. 1998; Chen and Naito 1999; Lisney and Collin 2008; Ullmann et al. 2012). In species from a range of vertebrate orders (including birds) for whom RGC topography has been assessed using both Nissl staining and retrograde labeling, the peak neuron densities and the overall retinal topography remain similar despite the inclusion of the displaced amacrine cells (e.g., Peterson and Ulinski 1979; Bravo and Pettigrew 1981; Hayes 1984; Collin 1999; Collin and Pettigrew 1988c; Pettigrew et al. 1988; Chen and Naito 1999; Bailes et al. 2006). Additionally, because neuron counts from the RGC layer are converted to neuron density (cells mm^{-2}) and then reduced to the square root for the purposes of calculating SRP (e.g., see Eq. 3), a relatively large difference in peak neuron density values results in only a small difference in terms of SRP (Pettigrew et al. 1988; Collin and Pettigrew 1989; Pettigrew and Manger 2008).

In phasianid birds, the displaced amacrine cells have been reported to account for almost none of the total population of neurons in the RGC layer in the Japanese quail (Budnik et al. 1984; Ikushima et al. 1986) to 20–35 % in the chicken (Ehrlich and Morgan 1980; Ehrlich 1981; Chen and Naito 1999) and their inclusion does not change the overall retinal topography (Ehrlich 1981; Chen and Naito 1999). In the chicken, amacrine cells account for approximately 13–30 % of the neurons in the *area centralis* (Ehrlich 1981; Chen and Naito 1999), while in the Japanese quail and the Indian peafowl (*Pavo cristatus*) this value is much lower ($\sim$0 and 5 %, respectively; Ikushima et al. 1986; Hart 2002). Even if we assume that 30 % of the neurons in the *area centralis* are displaced amacrine cells in all phasianids we investigated, and thus reduce our average peak cell density values for each species by this amount, our subsequent estimates of SRP across species are only reduced by 16 %, or $\sim$2 cycles/°. Given that estimates of peak SRP in birds vary from approximately 5–140 cycles/° (see below) and inter-individual variation in behavioral measures of SRP can suffer from having high individual variability (Pettigrew et al. 1988), such a difference in SRP is considered minimal (Pettigrew et al. 1988; Ghim and Hodos 2006; Pettigrew and Manger 2008).

In all seven species, the topographic distribution of neurons in the RGC layer consisted of a centrally positioned *area centralis* and a weak visual streak. Previous studies described a virtually identical pattern of retinal topography in the Japanese quail (Ikushima et al. 1986) as well as the domestic chicken (Ehrlich 1981; Straznicky and Chehade 1987) and the Indian peafowl (Hart 2002). This homogeneity in retinal topography across species that inhabit both open and enclosed habitats suggests that the terrain theory does not apply to phasianid birds. Although many animals across all of the major vertebrate orders conform to the terrain theory (e.g., Hughes 1977; Meyer 1977; Collin 1999, 2008; Lisney and Collin 2008; Lisney et al. 2012), it is likely that, in addition to the symmetry of a species' particular habitat, a range of other factors play a role in shaping a species' retinal topography, including the height of the eye/head above a substrate, ambient light levels, prey capture and feeding behavior, and the foraging strategies of potential predators (Hughes 1977, 1981; Collin 1999, 2008; Ahnelt et al. 2006; Schiviz et al. 2008). Thus, many factors, not just habitat, can affect the retinal topography of a species, and in the case of phasiands any or all of these factors may be more important than habitat type in determining retinal topography.

A central area of peak cell density (foveate or afoveate), like that observed in phasiands, is thought to be one of the most common forms of retinal organization in birds (Wood 1917; Meyer 1977; Dolan and Fernández-Juricic 2010). The *area centralis* (or fovea) is involved in monocular vision, viewing the central part of each eye's lateral visual field with a higher spatial resolving power (Meyer 1977; Ehrlich 1981). This enables phasianids, as well as other ground-foraging birds, to fixate food items and other objects monocularly and they only switch to frontal binocular vision to peck at an object of interest (Schlee 1983; Bischof 1988; Güntürkün et al. 1993). Presumably, this topographic arrangement of the retina, in combination with head movements, facilitates the identification of small food items on the ground (e.g., seeds, grains, shoots and insects) as well as other visually guided behaviors such as predator detection and identifying conspecifics (Necker 2007; Fernández-Juricic et al. 2011b), and does so equally in open and enclosed habitats.

Neuron number and SRP

Our estimates of the number and density of neurons in the RGC layer for each species were similar to those reported previously for the domestic chicken and the Japanese quail. Ehrlich (1981), Budnik et al. (1984), Ikushima et al. (1986) and Straznicky and Chehade (1987) estimated that the total number of neurons in the chicken and the Japanese quail range from 2.6 million and 1.3–2.0 million, respectively, which is similar to the 1.5–3.3 million for the seven species we examined. Similarly, peak neuron densities in the *area centralis* of the chicken range from 19,000 to 26,000 cells mm^{-2}; (Ehrlich 1981; Straznicky and Chehade 1987; Chen and Naito 1999), and our estimates ranged from ca. 22,000 to 29,000 cells mm^{-2}. Even the much higher peak neuron densities of the Japanese quail (ca. 35,000 cells mm^{-2}) are similar to those of previous studies (35,000–40,000 cells mm^{-2}, Budnik et al. 1984; Ikushima et al. 1986). Because the Japanese quail has a smaller eye (and thus a shorter PND) compared to the other phasianids we investigated, the increased peak neuron densities provide the Japanese quail with a peak anatomical SRP comparable to that of other phasianid birds (see below). In contrast, the Indian peafowl has both a relatively high peak neuron density (37,649 cells mm^{-2}) and a considerably larger eye (axial length = 19.4 mm), meaning that peak anatomical SRP in this species is about twice as high as that of any of the species we investigated (Hart 2002).

We estimated peak anatomical SRP to be approximately 10–13 cycles/° in the seven species we investigated. Because the RGC axons represent the only link between the eye and the brain, the peak values of anatomical SRP presented here represent the absolute upper possible threshold of SRP in these birds. Anatomical estimates of peak SRP are in close agreement with behavioral measures of SRP and the two are highly correlated (Kiltie 2000; Pettigrew et al. 1988; Pettigrew and Manger 2008). Thus, estimating SRP anatomically using the peak density of

neurons in the RGC layer and a measure of focal length has proved a valuable approach for predicting the visual capabilities of a wide range of species (e.g., Hughes 1977; Moroney and Pettigrew 1987; Pettigrew et al. 1988; Collin and Pettigrew 1989; Wathey and Pettigrew 1989; Hart 2002; Bailes et al. 2006; Lisney and Collin 2008; Pettigrew and Manger 2008; Dolan and Fernández-Juricic 2010; Pettigrew et al. 2010).

Estimates of peak SRP in the majority of birds studied to date range from ca. 5–40 cycles/° (Fite and Rosenfield-Wessels 1975; Moroney and Pettigrew 1987; Wathey and Pettigrew 1989; Hart 2002; Dolan and Fernández-Juricic 2010; Fernández-Juricic 2011a, b), with some Falconiform birds of prey having a much higher SRP (70–140 cycles/°) (Reymond 1985, 1987). Given this range, although our results indicate that there are significant differences in peak anatomical SRP among some phasianid species, we suggest that, as mentioned previously, differences in SRP such as those we have found among phasianids are minimal (Pettigrew et al. 1988; Ghim and Hodos 2006; Pettigrew and Manger 2008). SRP is largely dictated by eye size (Pettigrew et al. 1988; Collin and Pettigrew 1989; Lisney and Collin 2008; Dolan and Fernández-Juricic 2010), but there is evidence that SRP is related to foraging in birds. For example, our results are consistent with previous reports that ground-foraging species that feed on stationary prey items, such as songbirds and pigeons tend to have lower SRPs than diurnal predatory birds that feed on moving prey, like kingfishers and raptors (Reymond 1985, 1987; Moroney and Pettigrew 1987; Rounsley and McFadden 2005; Dolan and Fernández-Juricic 2010; Fernández-Juricic 2011a, b).

We could not identify a fovea in the highest neuron density area of any of our whole mounts. While it is possible to positively identify avian foveae in whole mounts (e.g., Bravo and Pettigrew 1981; Moroney and Pettigrew 1987; Inzunza et al. 1991; Coimbra et al. 2009; Lisney et al. 2012), the foveal region is fragile and can easily be damaged (Bravo and Pettigrew 1981; Lisney et al. 2012). Ideally, the presence or absence of a fovea should be confirmed using cross sections (Fernández-Juricic et al. 2011a), which we were unable to do with the specimens that we obtained. Despite this constraint, several studies have reported the absence of a fovea in phasianid and other galliform species (Wood 1917; Walls 1942; Ehrlich 1981; Morris 1982; Budnik et al. 1984; Chen and Naito 1999; Hart 2002). Ikushima et al. (1986) did report the presence of a fovea in the Japanese quail, but the fovea was described as being 'shallow'. Well-developed foveae have been associated with rapid flight and the capture of moving prey in birds (Meyer 1977; Fite and Rosenfield-Wessels 1975; Inzunza et al. 1991), which is consistent with the finding that phasianid birds either lack or have a poorly developed fovea, given that they are ground dwellers and feed on stationary prey items.

The majority (6/7) of the species we examined only had an *area centralis*, but the Japanese quail had a dorso-temporal extension of increased neuron density and, in two specimens, a second, putative high density area that may be an *area dorsalis* was identified. Our observations are corroborated by previous studies of Japanese quail; Budnik et al. (1984) identified an *area dorsalis*, but Ikushima et al. (1986) did not. Similarly, while an *area dorsalis* was reported to be present in the chicken by Chen and Naito (1999), Ehrlich (1981) only reported a dorso-temporal extension of increased neuron density. Other ground-foraging birds, such as the pigeon (Binggeli and Paule 1969; Hayes and Holden 1983) and the jungle crow (Rahman et al. 2006), also have both central and dorso-temporal areas of high neuron density. An *area dorsalis* may be an adaptation for viewing the part of the frontal visual field in front of and just below the beak, so facilitating binocular vision and visually guided pecking behaviors that are important in feeding (Binggeli and Paule 1969; Zeigler et al. 1993; Hart 2002). Given that all phasianid birds are ground foragers, it is unclear why some species appear to have an *area dorsalis*, while others do not, or why this retinal specialization does not appear to be present in all individuals within a species. It is possible that this may be a result of be natural inter- and intra-specific variation in the organization of the retina among phasianids. Alternatively, it could be due to an artifact of the whole mounting process, as a tear or an orientation cut in the dorso-temporal retina could make an *area dorsalis* difficult to identify (Ullmann et al. 2012). In addition, the chicken and the Japanese quail have been heavily domesticated (del Hoyo et al. 1994; Appleby et al. 2004) and it has also been suggested that domestication may have played a role in altering retinal organization in these species (Walls 1942; Budnik et al. 1984; Ikushima et al. 1986), although no mechanism has been suggested.

Our data suggest that eye morphology is adapted to variation in ambient light levels associated with enclosed and open habitats in phasianid birds. While previous studies have shown a close relationship between activity pattern and eye morphology in birds (Hall and Ross 2007; Iwaniuk et al. 2010; Lisney et al. 2012), this is the first study to show such a relationship between habitat and eye morphology, and further studies focused on different avian taxa will be required to confirm the extent to which such habitat-specific variation in ambient light levels influences eye morphology across birds in general. Regarding retinal topography, contrary to our prediction based on Hughes' (1977) terrain theory, we found no evidence of habitat-specific variation in retinal topography among phasianid species from open and enclosed habitats. While a wide

range of vertebrates have been found to conform to the terrain theory, this study serves as an important illustration that other factors in addition to the symmetry of a species' particular habitat, such as the visual demands of a particular foraging strategy, can play a role in shaping retinal topography.

Acknowledgments This study was funded by Natural Sciences and Engineering Research Council of Canada (NSERC) Discovery Grants to DRW and ANI. We wish to thank Bill Young, Jodi Saucier, Greg Sanbourne, George Iwaniuk and Udo Hannebaum for providing specimens for our study and Maxime Garcia for assistance in trapping ruffed grouse. The grouse were collected under Alberta Department of Sustainable Resource Development Research and Collection Permits 47079 and 47080. All of our methods adhered to Canadian Council for Animal Care Guidelines and were approved by the University of Lethbridge Animal Welfare Committee.

References

Ahnelt PK, Schubert C, Kübber-Heiss A, Schiviz A, Anger E (2006) Independent variation of retinal S and M cone photoreceptor topographies: a survey of four families of mammals. Vis Neurosci 23:429–435

Appleby MC, Mench JA, Hughes BO (2004) Poultry behaviour and welfare. CABI Publishing, Wallingford

Archibald HL (1976) Spring drumming patterns of ruffed grouse. Auk 93:808–829

Bailes HJ, Trezise AEO, Collin SP (2006) The number, morphology, and distribution of retinal ganglion cells and optic axons in the Australian lungfish *Neoceratodus forsteri* (Krefft 1870). Vis Neurosci 23:257–273

Bergerud AT, Gratson MW (eds) (1988) Adaptive strategies and population ecology of northern grouse. In: Theory and synthesis, vol 2. University of Minnesota Press, Minneapolis

Binggeli RL, Paule WJ (1969) The pigeon retina: quantitative aspects of optic nerve and ganglion cell layer. J Comp Neurol 137:1–18

Bischof H-J (1988) The visual field and visually guided behavior in the zebra finch (*Taeniopygia guttata*). J Comp Physiol A 163: 329–337

Boire D, Dufour JS, Theoret H, Ptito M (2001) Quantitative analysis of the retinal ganglion cell layer in the ostrich, *Struthio camelus*. Brain Behav Evol 58:343–355

Bravo H, Pettigrew JD (1981) The distribution of neurons projecting from the retina and visual cortex to the thalamus and tectum opticum of the barn owl, *Tyto alba*, and burrowing owl, *Speotyto cunicularia*. J Comp Neurol 199:419–441

Budnik V, Mpodozis J, Varela FJ, Maturana HR (1984) Regional specialization of the quail retina: ganglion cell density and oil droplet distribution. Neurosci Lett 51:145–150

Chen Y, Naito J (1999) A quantitative analysis of the cells in the ganglion cell layer of the chick retina. Brain Behav Evol 53:75–86

Christisen GC (1970) The chukar partridge: its introduction, life history and management. Biological Bulletin No. 4, Nevada Department of Fish and Game, Reno

Coimbra JP, Trévia N, Marceliano ML, da Silveira Andrade-Da-Costa BL, Picanço-Diniz CW, Yamada ES (2009) Number and distribution of neurons in the retinal ganglion cell layer in relation to foraging behaviors of tyrant flycatchers. J Comp Neurol 514:66–73

Collin SP (1999) Behavioural ecology and retinal cell topography. In: Archer SN, Djamgoz MBS, Loew ER, Partridge JC, Vellarga S (eds) Adaptive mechanisms in the ecology of vision. Kluwer, Dordrecht, pp 509–535

Collin SP (2008) A web-based archive for topographic maps of retinal cell distribution in vertebrates. Clin Exp Optom 91:85–95

Collin SP, Pettigrew JD (1988a) Retinal topography in reef teleosts. I. Some species with well-developed areae but poorly-developed streaks. Brain Behav Evol 31:269–282

Collin SP, Pettigrew JD (1988b) Retinal topography in reef teleosts. II. Some species with prominent horizontal streaks and high-density areae. Brain Behav Evol 31:283–295

Collin SP, Pettigrew JD (1988c) Retinal ganglion cell topography in teleosts: a comparison between Nissl-stained material and retrograde labelling from the optic nerve. J Comp Neurol 276:412–422

Collin SP, Pettigrew JD (1989) Quantitative comparison of the limits on visual spatial resolution set by the ganglion cell layer in twelve species of reef teleosts. Brain Behav Evol 34:184–192

Collin SP, Hoskins RV, Partridge JC (1998) Seven retinal specializations in the tubular eye of the deep-sea pearleye, *Scopelarchus michaelsarsi*: a case study in visual optimization. Brain Behav Evol 51:291–314

Corfield JR, Gsell AC, Brunton D, Heesy CP, Hall MI, Acosta ML, Iwaniuk AI (2011) Anatomical specializations for nocturnality in a critically endangered parrot, the kakapo (*Strigops habroptilus*). PLoS One 6:e22945

Crowe TM, Bowie RCK, Blommer P, Mandiwana TG, Hedderson TAJ, Randi E, Pereira SL, Wakeling J (2006) Phylogenetics, biogeography and classification of, and character evolution in, gamebirds (Aves: Galliformes): effects of character exclusion, data partitioning and missing data. Cladistics 22:495–532

del Hoyo J, Elliott A, Sargatal J (eds) (1994) Handbook of the birds of the world. New world vultures to guineafowl, vol 2. Lynx Edicions, Barcelona

Dolan T, Fernández-Juricic E (2010) Retinal ganglion cell topography of five species of ground-foraging birds. Brain Behav Evol 75:111–121

Ehrlich D (1981) Regional specialization of the chick retina as revealed by the size and density of neurons in the ganglion cell layer. J Comp Neurol 195:643–657

Ehrlich D, Morgan IG (1980) Kainic acid destroys displaced amacrine cells in post-hatch chicken retina. Neurosci Lett 17:43–48

Endler JA (1993) The color of light in forests and its implications. Ecol Monogr 63:1–27

Fernández-Juricic E, Moore BA, Doppler M, Freeman J, Blackwell BF, Lima SL, DeVault TL (2011a) Testing the terrain hypothesis: Canada geese see their world laterally and obliquely. Brain Behav Evol 77:147–158

Fernández-Juricic E, Gall MD, Dolan T, O'Rourke C, Thomas S, Lynch JR (2011b) Visual systems and vigilance behaviour of two ground-foraging avian prey species: white-crowned sparrows and California towhees. Anim Behav 81:705–713

Fite KV, Rosenfield-Wessels S (1975) A comparative study of deep avian foveas. Brain Behav Evol 12:97–115

Foster RG, Korf H-W, Schalken JJ (1987) Immunocytochemical markers revealing retinal and pineal but not hypothalamic photoreceptor systems in the Japanese quail. Cell Tissue Res 248:161–167

Fowler J, Cohen L (1990) Practical statistics for field biology. Wiley, Chichester

Ghim MM, Hodos W (2006) Spatial contrast sensitivity of birds. J Comp Physiol A 192:523–534

Gullion GW (1965) Improvements in methods for trapping and marking ruffed grouse. J Wildl Manage 29:109–116

Gullion GW (1984) Grouse of the north shore. Willow Creek Press, Oshkosh

Gundersen HJG (1977) Notes on the estimation of the numerical density of arbitrary particles: the edge effect. J Microsc 111:219–223

Güntürkün O, Miceli D, Watanabe M (1993) Anatomy of the avian thalamofugal pathway. In: Zeigler HP, Bischof H-J (eds) Vision, brain, and behavior in birds. MIT Press, Cambridge, pp 115–135
Hall MI, Ross CF (2007) Eye shape and activity pattern in birds. J Zool 271:437–444
Hart NS (2002) Vision in the peafowl (Aves: *Pavo cristatus*). J Exp Biol 205:3925–3935
Hayes BP (1984) Cell populations of the ganglion cell layer: displaced amacrine and matching amacrine cells in the pigeon retina. Exp Brain Res 56:565–573
Hayes BP, Brooke MD (1990) Retinal ganglion cell distribution and behavior in Procellariiform seabirds. Vision Res 30:1277–1289
Hayes BP, Holden AL (1983) The distribution of displaced ganglion cells in the retina of the pigeon. Exp Brain Res 49:181–188
Howard CV, Reed MG (2005) Unbiased stereology: three-dimensional measurement in microscopy, 2nd edn. BIOS Scientific Publishers, Abingdon
Hughes A (1975) A comparison of retinal ganglion cell topography in the plains and tree kangaroo. J Physiol (Lond) 244:61–63
Hughes A (1977) The topography of vision in mammals of contrasting lifestyles: comparative optics and retinal organization. In: Cresitelli F (ed) Handbook of sensory physiology, vol VIII/5. Springer, Berlin, pp 613–756
Hughes A (1981) One brush tailed possum can browse as much pasture as 0.06 sheep which may indicate why this "arboreal" animal has a visual streak: some comments on the "terrain" theory. Vis Res 21:957–958
Hughes A (1985) New perspectives in retinal organization. In: Osbourne NN, Chader G (eds) Progress in retinal research. Pergamon Press, New York, pp 243–313
Ikushima M, Watanabe M, Ito H (1986) Distribution and morphology of retinal ganglion cells in the Japanese quail. Brain Res 376:320–334
Inzunza O, Bravo H, Smith RL, Angel M (1991) Topography and morphology of retinal ganglion cells in Falconiforms: a study on predatory and carrion-eating birds. Anat Rec 229:271–277
Iwaniuk AN, Heesy CP, Hall MI (2010) Morphometrics of the eyes and orbits of the nocturnal swallow-tailed gull (*Creagrus furcatus*). Can J Zool 88:855–865
Johnsgard PA (1973) Grouse and quails of North America. University of Nebraska, Lincoln
Kiltie RA (2000) Scaling of visual acuity with body size in mammals and birds. Funct Ecol 2000(14):226–234
Kirk EC (2004) Comparative morphology of the eye in primates. Anat Rec 281A:1095–1103
Kirk EC (2006) Eye morphology in cathemeral lemurids and other mammals. Folia Primatol (Basel) 77:27–49
Kolm N, Stein RW, Mooers AØ, Verspoor JJ, Cunningham JA (2006) Can sexual selection drive female life histories? A comparative study on Galliform birds. J Evol Biol 20:627–638
Lessells CM, Boag PT (1987) Unrepeatable repeatabilities: a common mistake. Auk 104:116–121
Lisney TJ, Collin SP (2008) Retinal ganglion cell distribution and spatial resolving power in elasmobranchs. Brain Behav Evol 72:59–77
Lisney TJ, Iwaniuk AN, Bandet MV, Wylie DW (2012) Eye shape and retinal topography in owls (Aves: Strigiformes). Brain Behav Evol 79:218–236
Martin GR (1982) An owl's eye: schematic optics and visual performance in *Strix aluco* L. J Comp Physiol A 145:341–349
Martin GR (1994) Form and function in the optical structure of bird eyes. In: Green PR (ed) Davies MNO. Springer, Berlin, pp 5–34
Meyer DB (1977) The avian eye and its adaptations. In: Cresitelli F (ed) Handbook of sensory physiology, vol VIII/5. Springer, Berlin, pp 549–611
Meyer DB, May HC Jr (1973) The topographic distribution of rods and cones in the adult chicken retina. Exp Eye Res 17:347–355
Moroney MK, Pettigrew JD (1987) Some observations on the visual optics of kingfishers (Aves, Coraciformes, Alcedinidae). J Comp Physiol A 160:137–149
Morris VB (1982) An afoveate area centralis in the chick retina. J Comp Neurol 210:198–203
Necker R (2007) Head-bobbing of walking birds. J Comp Physiol A 193:1177–1183
Oehme H (1961) Vergleichend-histologische Untersuchungen an der Retina von Eulen. Zool Jb Anat 79:439–478 (Article in German)
Ovington JD, Madgwick HAI (1955) A comparison of light in different woodlands. Forestry 28:141–146
Peterson EH, Ulinski PS (1979) Quantitative studies of retinal ganglion cells in a turtle, *Pseudemys scripta elegans*. 1. Number and distribution of ganglion cells. J Comp Neurol 186:17–42
Pettigrew JD, Manger PR (2008) Retinal ganglion cell density of the black rhinoceros (*Diceros bicornis*): calculating visual resolution. Vis Neurosci 25:215–220
Pettigrew JD, Dreher B, Hopkins CS, McCall MJ, Brown M (1988) Peak density and distribution of ganglion cells in the retinae of microchiropteran bats: implications for visual acuity. Brain Behav Evol 32:39–56
Pettigrew JD, Bhagwandin A, Haagensen M, Manger PR (2010) Visual acuity and heterogeneities of retinal ganglion cell densities and the tapetum lucidum of the African elephant *(Loxodonta africana)*. Brain Behav Evol 75:251–261
Quinn GP, Keough MJ (2002) Experimental design and data analysis for biologists. Cambridge University Press, Cambridge
Rahman ML, Sugita S, Aoyama M, Sugita S (2006) Number, distribution and size of retinal ganglion cells in the jungle crow (*Corvus macrorhynchos*). Anat Sci Int 81:253–259
Rahman ML, Aoyama M, Sugita S (2007) Regional specialization of the tree sparrow *Passer montanus* retina: ganglion cell density and oil droplet distribution. Ornithol Sci 6:95–105
Rasband WS (1997–2011) Image J. US National Institutes of Health, Bethesda
Reymond L (1985) Spatial visual acuity of the eagle *Aquila audax*: a behavioural, optical and anatomical investigation. Vis Res 25:1477–1491
Reymond L (1987) Spatial visual acuity of the falcon, *Falco berigora*: a behavioural, optical and anatomical investigation. Vis Res 27:1859–1874
Rojas LM, Ramirez Y, McNeil R, Mitchell M, Marin G (2004) Retinal morphology and electrophysiology of two Caprimulgiformes birds: the cave-living and nocturnal oilbird (*Steatornis caripensis*), and the crepuscularly and nocturnally foraging common pauraque (*Nyctidromus albicollis*). Brain Behav Evol 64:19–33
Rounsley KJ, McFadden SA (2005) Limits of visual acuity in the frontal field of the rock pigeon (*Columba livia*). Perception 34:983–993
Schaeffel F, Howland HC (1989) Visual optics in normal and ametropic chickens. Clin Vision Sci 3:83–98
Scheaffer RL, Mendenhall W, Ott L (1996) Elementary survey sampling, 5th edn. PWS-Kent, Boston
Schiviz AN, Ruf T, Kuebber-Heiss A, Schubert C, Ahnelt PK (2008) Retinal cone topography of artiodactyl mammals: influence of body height and habitat. J Comp Neurol 507:1336–1350
Schlee MA (1983) An experimental study of prey-attack behavior in the European blackbird *Turdus m. merula* L. Z Tierpsychol 61:203–224
Schmitz C, Hof PR (2000) Recommendations for straightforward and rigorous methods of counting neurons based on a computer simulation approach. J Chem Neuroant 20:93–114

Schmitz L, Wainwright PC (2011) Nocturnality constrains morphological and functional diversity in the eyes of reef fishes. BMC Evol Biol 11:338

Snyder AW, Miller WH (1977) Photoreceptor diameter and spacing for highest resolving power. J Opt Soc Am 67:696–698

Stone J (1981) The wholemount handbook: a guide to the preparation and analysis of retinal wholemounts. Clarendon Press, Sydney

Straznicky C, Chehade M (1987) The formation of the area centralis of the retinal ganglion cell layer of the chick. Development 100:411–420

Ullmann JFP, Moore BA, Temple SH, Fernández-Juricic E, Collin SP (2012) The retinal wholemount technique: a window to understanding the brain and behaviour. Brain Behav Evol 79:26–44

Veilleux CC, Lewis RJ (2011) Effects of habitat light intensity on mammalian eye shape. Anat Rec 294:905–914

Walls GL (1942) The vertebrate eye and its adaptive radiation. Cranbrook Institute of Science, Bloomfield Hills

Warrant E (2004) Vision in the dimmest habitats on Earth. J Comp Physiol A 190:765–789

Wathey JC, Pettigrew JD (1989) Quantitative analysis of the retinal ganglion cell layer and optic nerve of the barn owl *Tyto alba*. Brain Behav Evol 33:279–292

Wood CA (1917) The fundus oculi of birds, especially as viewed by the ophthalmoscope: a study in comparative anatomy and physiology. Lakeside Press, Chicago

Zeigler HP, Bischof H-J (eds) (1993) Vision, brain, and behavior in birds. MIT Press, Cambridge

Zeigler HP, Jäger R, Palacios AG (1993) Sensorimotor mechanisms and pecking in the pigeon. In: Zeigler HP, Bischof H-J (eds) Vision, brain, and behavior in birds. MIT Press, Cambridge, pp 265–283